THE JOURNAL OF PHYSICAL CHEMISTRY C

Article

pubs.acs.org/JPCC

Critical Effect of Segmental Dynamics in Polybutadiene/Clay Nanocomposites Characterized by Solid State ^{1}H NMR Spectroscopy

Yun Gao,[†] Rongchun Zhang,[‡] Weifeng Lv,[§] Qingjie Liu,[§] Xiaoliang Wang,*[,†] Pingchuan Sun,[‡] H. Henning Winter,[∥] and Gi Xue[†]

[†]Key Laboratory of High Performance Polymer Materials and Technology (Nanjing University), Ministry of Eduction., Department of Polymer Science and Engineering, School of Chemistry and Chemical Engineering, Nanjing University, Nanjing, 210093, P. R. China

[‡]Key Laboratory of Functional Polymer Materials of Ministry of Education, College of Chemistry and School of Physics, Nankai University, Tianjin, 300071, P. R. China

[§]Research Institute of Petroleum Exploration & Development, PetroChina, Beijing, 100083, P. R. China

[∥]Department of Chemical Engineering and Department of Polymer Science and Engineering, University of Massachusetts, Amherst, Massachusetts 01003, United States

ABSTRACT: The segmental dynamics of rigid, intermediate, and mobile molecular components in carboxyl terminated polybutadiene (CTPB)/organo−clay (C_{18}−clay) systems was characterized by fully refocused ^{1}H NMR FID. In addition, ^{1}H DQ NMR experiments allowed semiquantitative monitoring of changes in segmental dynamics near the interface. Both methods suggest a critical concentration of 60 wt % CTPB, indicating a saturation effect for the surface-adsorbed polymer. While the critical concentration value of a polymer/clay system can be measured in several ways, this is its first direct evidence at the molecular scale. The polymer−clay interaction is found to profoundly change with the removal of the CTPB end group or the organic modifier on the clay surface thus impacting the polymer segmental dynamics near the clay surface. In C_{18}−clay by itself, with increasing temperature, the dynamic behavior of surface modifier changes from homogeneous to heterogeneous, on the basis of which the nonreversible exfoliation process of CTPB/clay nanocomposites could be explained at the molecular level. Based on the ^{1}H NMR results, a tentative model was proposed to illustrate the evolution of the structure and segmental dynamics in CTPB/organo−clay nanocomposites.

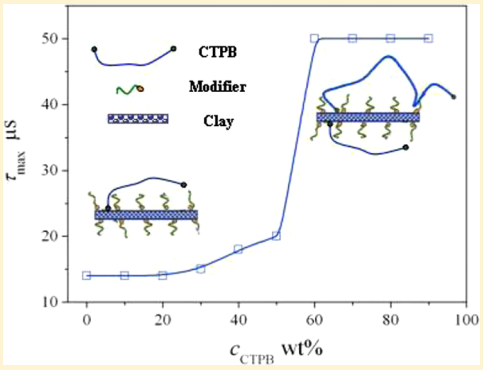

INTRODUCTION

Polymer/clay nanocomposites are attractive not only for their obvious technological potential as composites[1−5] but also as a meaningful model system for studying the fundamentals of nanoscopically confined macromolecules.[6−8] Clay particles are layered silicates with nanometer thick sheets. When immersed in a matrix polymer, provided that conditions are favorable, macromolecules can diffuse in between the silica sheets. The incorporation of polymer chains increases the spacing between clay sheets (intercalation) and may even exfoliate the clay stacks completely. The polymer−clay interaction at the organic−inorganic interface and the confinement between clay sheets affect the polymer segmental dynamics.[9−12] The understanding of polymer segmental dynamics in confined environments will be crucial for optimal processing and controlled structure development for these nanocomposites.[2,6,13−15] Chain conformation and dynamics of polymers have been probed with a variety of techniques including rheology,[14,16,17] thermal analysis,[18,19] solid-state NMR,[20−28] and dielectric spectroscopy.[29−31] The experimental observations guided computer simulations of the relevant molecular dynamics[7] and possible molecular conformations.[32] Diverse phase diagrams of polymer/clay nanocomposites have been proposed.[12,33−35] However, still missing is the molecular level understanding of the polymer segmental dynamics near clay surfaces, which is the key for controlling the property of the final nanocomposites.

Solid state NMR spectroscopy has been established as a powerful technique to observe structure and segmental dynamics of polymers at the molecular level.[36−44] In principle, molecular mobility can be deduced from simple FID signals where a fast or slow decay indicates the presence of rigid or mobile components, respectively.[45] In comparison, proton multiple quantum NMR (MQ NMR) mostly probes molecular motions that involve a large number of segments up to the level of the whole chain, which dominates the mechanical properties of soft polymeric systems.[39] Graf et al. used ^{1}H MQ NMR under fast magic angle spinning (MAS) to elucidate the nature

Received: February 7, 2014
Revised: February 18, 2014
Published: February 19, 2014

   dx.doi.org/10.1021/jp5013472 | J. Phys. Chem. C 2014, 118, 5606−5614

of the polymer segmental dynamics in polybutadiene[46] and cross-linked poly(styrene-*co*-butadiene)[47] melt far above the glass transition with site resolution. Blümich et al.[48] used the ^{1}H double quantum (DQ) NMR method at static conditions to study soft materials such as PDMS grafted onto silica surfaces[49] or PDMS ultrathin films.[50] As shown in previous examples of grafted chains,[49,50] the exact quantification of the related dipolar couplings is made complicated by an ill-defined intensity scale, which does not clearly separate relaxation from intermediate motions.[39] Saalwächter et al. introduced a reference signal by changing the phase cycling and were able to quantitatively analyze the segmental dynamics and structural constraints in polymeric soft materials utilizing Baum-Pines sequences[51] with a benchtop low-field NMR spectrometer.[39,52−56] Their quantitative study on chemical gelation by ^{1}H MQ NMR[52] agreed well with rheological and optical measurements.[57−59] Zhang et al. studied the heterogeneous network structure and hydrogen bonding dynamics as well as the significant aging properties of the supramolecular self-healing rubber utilizing DQ NMR and T_2 relaxometry.[45] Also, Litvinov et al. utilized DQ NMR and T_2 relaxometry to study the rubber−filler interaction in carbon black and silica filled rubbers, and quantitative information about immobilization of rubber chains on the surface of fillers was obtained.[60−62]

The segmental dynamics near clay surfaces had been hypothesized to play an important role in a new class of telechelic polybutadiene/clay nanocomposite physical gels.[63−67] We found that highly anisotropic, organically modified silicates (C_{18}−clay) rapidly exfoliate when embedded in dicarboxyl-terminated 1,4-polybutadiene (CTPB) or hydroxyl-terminated 1,4-polybutadiene (HTPB), up to a clay concentration of 10 wt %.[65] Rheological experiments, after having mixed the clay into the polymer, identified two vastly different structuring processes of intercalation and exfoliation and indicated that the structural ripening process was governed by regular rheological patterns which might be typical for physical gelation.[67] Sun et al. had used deuterated benzene as a probe molecule in ^{2}H NMR spectroscopy to characterize organo−clay dispersion quality and relevant confinement effects in these nanocomposites.[68] Until now, a detailed understanding of the evolution of segmental dynamics with CTPB concentrations and the relationship between the structure and dynamics at a molecular level in polymer/clay nanocomposites remained an open challenge.[39]

The current study aims to understand the complex segmental dynamics of macromolecules which are confined in the narrow space between two-dimensional clay sheets of polybutadiene (PB) /clay nanocomposites. CTPB/C_{18}−clay served as a model system. Segmental dynamics were studied with ^{1}H NMR at static conditions. The dynamical heterogeneity was quantitatively described in a model which groups fractions as rigid, intermediate, or mobile components as well as the corresponding spin−spin relaxation time through fitting FID decay signals. The polymer−clay interaction was controlled by the functionalized end group and/or surface modification.[11] We took advantage of ^{1}H DQ NMR for studying this segmental dynamics of PB (with or without functionalized end group) which interacts with clay (with or without modifier) at different PB concentrations and temperatures (much above the glass transition temperature of PB of about −70 °C). On the basis of the ^{1}H NMR results, a tentative model was proposed to elucidate the evolution of the structure and segmental dynamics in the CTPB/C_{18}−clay nanocomposites.

EXPERIMENTAL SECTION

Materials. Dicarboxyl-terminated 1,4-polybutadiene oligomers (CTPB) of M_n = 4200 g/mol and the 1,2-polybutadiene oligomer (PB) of M_n = 3300 g/mol, without functionalized end groups, were purchased from Aldrich Chemical Co. The organo−clay (C_{18}−clay) was pristine montmorillonite (MMT, Tianjin Organic Clay Corp. China, cation exchange capacity of 1 mequiv/g) that was modified with octadecyltrimethylammonium chloride as described elsewhere.[65] TGA result showed 35.0 wt % modifier was on the clay sheet, this will be used as proton calibration while CTPB added.

Preparation of Structurally Equilibrated Samples. Desired amounts of CTPB (or PB) and C_{18}−clay (or MMT) were combined by first dissolving the polymer in purified chloroform and then adding the clay. The mixture was homogenized by applying ultrasound, then exposing it to room temperature until the chloroform had evaporated, and annealing it in vacuum at 80 °C overnight to obtain a structurally stable sample.[8,69] TGA results showed no weight loss before 100 °C, suggested no water left in all of the samples, especially the samples with MMT. All concentration values in the text refer to CTPB or PB content. In our previous work, we had shown that C_{18}−clay could fully exfoliate at high CTPB concentration, c_{CTPB} > 90 wt %, while composites with less CTPB were only partially exfoliated or intercalated. PB/MMT remained a suspension of macroscopic clay particles in PB. PB/C_{18}−clay, CTPB/MMT samples reached some intermediate structure (intercalation).[63,65]

Excluded from the present study is the slowdown of the macromolecules during gelation which would require time-resolved measurements to accommodate for the evolving connectivity. This would exceed the focus of this study which concentrates on stable structural conditions and the polymer−clay interactions.

^{1}H NMR Experiments. The measurements were performed in a Bruker Minispec mq20 low-field spectrometer at 20 MHz proton resonance frequency with a typical $\pi/2$ pulse length of about 3 μs and receiver dead time of about 13 μs. A BVT-3000 controlled the temperature with an accuracy of ±0.1 K. Magic-sandwich echo (MSE, shown in Figure 1a)[56] could well refocus the initial FID signal, which gets lost in the single pulse experiment due to the dead time problem of the spectrometer.

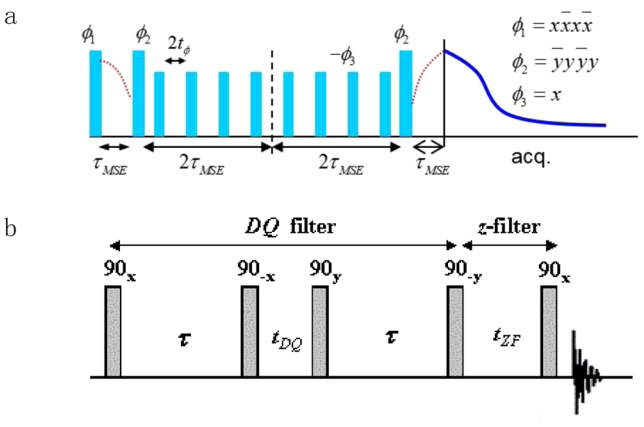

Figure 1. (a) Magic-sandwich echo (MSE) pulse sequence for refocusing the loss of rigid-phase signal due to the dead time. (b) The ^{1}H DQ five pulse sequence.[70]

dx.doi.org/10.1021/jp5013472 | J. Phys. Chem. C 2014, 118, 5606−5614

A Hahn echo pulse sequence could well eliminate magnetic field inhomogeneity as well as refocus chemical shift anisotropy. We combined the MSE FID at short acquisition time (~80 μs) with ^{1}H Han echo decay signal at long echo time (80−10^6 μs) to obtain a fully recovered FID. Then, the FID shape was fitted to a linear combination of Weibull and two exponential function as suggested by Litvinov et al.:[62]

$$A(t) = A_0[f_{\text{rigid}} \exp(-t/T_{2,\text{rigid}})^a + f_{\text{inter}} \exp(-t/T_{2,\text{inter}}) + f_{\text{mobile}} \exp(-t/T_{2,\text{mobile}})] \quad (1)$$

where f_{rigid}, f_{inter}, and f_{mobile} were the fractions for the rigid, intermediate, and mobile components with corresponding apparent relaxation times $T_{2,\text{rigid}}$, $T_{2,\text{inter}}$, and $T_{2,\text{mobile}}$.

^{1}H DQ NMR experiments were performed at a proton frequency of 399.7 MHz on a Varian Infinityplus-400 wide-bore (89 mm) NMR spectrometer equipped with a temperature control unit using a 7.5 mm MAS probe head under static conditions. Although the Baum-Pines DQ sequence was reported to produce pure dipolar Hamilitonian,[39,51] it could only excite the DQ signals of mobile components due to the length limit of the pulse sequence, ~100 μs in minimum. Therefore, in order to observe DQ signals of the rigid components as well as of the intermediate polymer/clay interface, a two-pulse segment (90°−τ−90°) was adopted for the excitation and reconversion of DQ signals. This procedure is able to excite DQ signals among strong dipolar-coupled protons with a relatively short excitation time,τ. The 90° pulse width, the evolution, and Z-filter periods were 6, 5, and 30 μs, respectively. The DQ build-up curves were normalized to the integral intensity of the NMR signal after a 90° pulse.

RESULTS

Overview from the Fully Refocused FIDs. The interaction of polymer and clay results in heterogeneous mobility of the nanocomposites: relative rigidity on the surface and mobility away from the surface. Such molecular mobility differences show up in simple FID signals.[45] A fast decay indicates the presence of rigid components, while a slow decay is the response of mobile components. In the single pulse experiment, the spectrometer looses the initial part of the FID signals due to a long dead time, and the recorded fraction of rigid components would be underestimated in the final FID decomposition analysis. To overcome this, a MSE sequence was used to refocus the missing initial FID signals. A problem also arises at long acquisition times where the magnetic field inhomogeneity may result in a decay of FID and, thus, would obscure our analysis. Herein, Hahn echo was also utilized to record the FID signal decay with increasing echo time (80−10^6 μs), as it was able to well eliminate the magnetic field inhomogeneity and refocus the chemical shift anisotropy. A fully refocused FID with complete shape could be obtained through a combination of MSE FID and Hahn echo decay. Fitting the decay to a multicomponent model provided quantitative information of components with different mobility in the system.

The fully refocused FIDs of CTPB/C_{18}−clay nanocomposites are shown in Figure 2. With increasing CTPB amount, the FID decayed more and more slowly. A quantitative fit to the above model, eq 1, provided the T_2 value and the relative fraction of the relaxation components of CTPB/C_{18}−clay as plotted in Figure 3a and 3b.

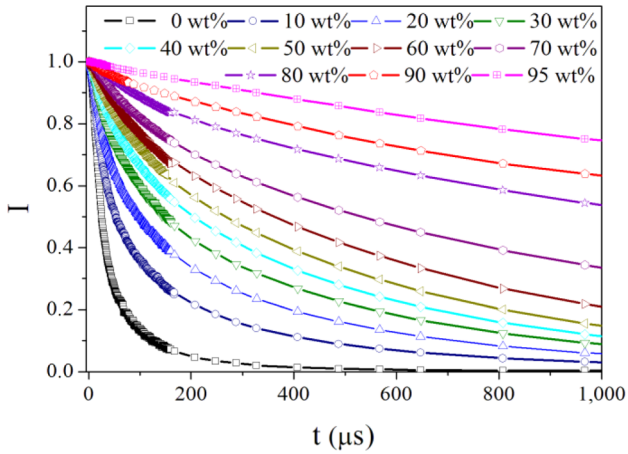

Figure 2. Fully refocused ^{1}H NMR FID of CTPB/C_{18}−clay with different CTPB contents at 30 °C. We only presented the decay data until 1000 μs for clear comparison. The experiments were recorded up to 4 × 10^6 μs.

No mobile signal could be extracted from the FID of pure C_{18}−clay (c_{CTPB} = 0 wt %) because all of the modifier molecules were tightly attached to the clay surface. The rigid components are attributed to the modifier head on the clay surface, whereas the intermediate components originate from the modifier tail somewhat further away from the clay surface. In order to compare the contribution from CTPB, we plot the dash lines stand for ideal rigid (black) and intermediate (blue) fractions from pure C_{18}−clay, assuming that the C_{18}−clay has no interaction with CTPB. The dash lines are calibrated by excluding inorganic clay sheet based on TGA result.

In the range of 10 ≤ c_{CTPB} ≤ 50 wt %, apart from the rigid and intermediate components, a mobile phase is expected to appear due to the presence of the CTPB macromolecules. However, by use of eq 1 we found that all three T_2 values increased only slightly. Even the $T_{2,\text{mobile}}$ value in this range was still much lower than the corresponding bulk value (around 5 s). These observations suggest that the CTPB macromolecules were all in a confined state; that is, all CTPB was intercalated inside the clay galleries or tightly attached on the outside. This changed significantly when further increasing c_{CTPB}:

- f_{rigid} decreased dramatically at higher c_{CTPB}, which is much lower than the ideal rigid dash line. This suggests a dramatic softening of the C_{18}-modifier that is attached to the clay surface.
- f_{inter} decreased nearly linearly with CTPB content which is much higher than the ideal intermediate dash line. f_{inter} expresses the mobility of two components, the modifier tail away from the clay surface and CTPB molecules confined by the clay surface.
- f_{mobile} grew steeply with increasing c_{CTPB} because of the decreasing clay fraction. The mobile fraction is solely attributed to the mobile CTPB.

In the higher range of c_{CTPB} ≥ 60 wt %, no more rigid component could be extracted by means of eq 1. The absence of rigid components agrees with the first τ_{max} position variation in Figure 7 and will be discussed in the following section. With increasing c_{CTPB}, $T_{2,\text{inter}}$ increased slowly at first but then grows significantly. In previous experiments,[65] we found a mixture of intercalated and exfoliated structure in this range, and a fully exfoliated structure for c_{CTPB} > 90 wt %.

dx.doi.org/10.1021/jp5013472 | J. Phys. Chem. C 2014, 118, 5606−5614

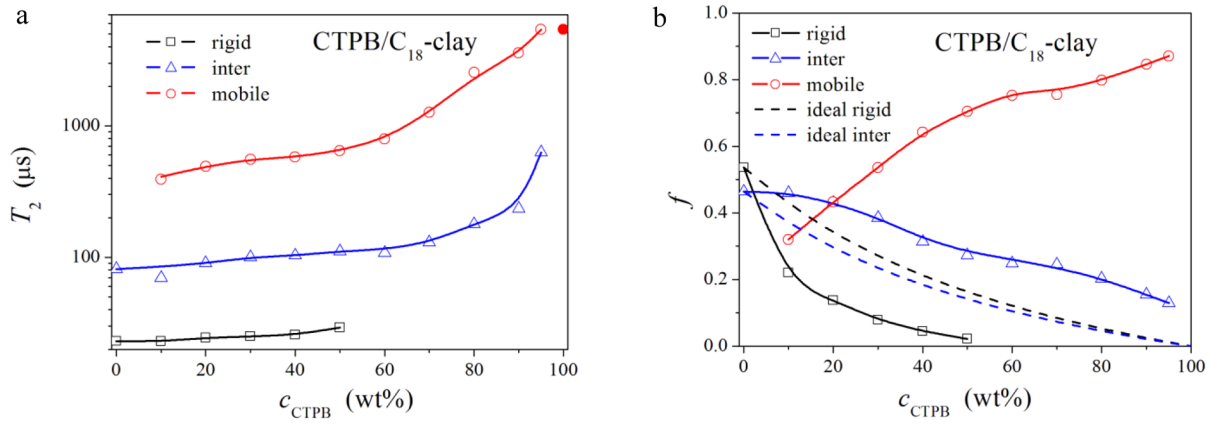

Figure 3. Concentration dependence of (a) T_2 and (b) the rigid, intermediate, and mobile fraction in CTPB/C_{18}–clay. T_2 of pure CTPB is plotted with a filled symbol for comparison. The dash lines stand for ideal rigid (black) and intermediate (blue) fractions from pure C_{18}–clay without interaction with CTPB.

The data suggest a critical c_{CTPB}, at which exfoliation sets in: the turning point of $T_{2,inter}$ (c_{CTPB} = 80 wt %) suggests the appearance of exfoliated clay sheets. New mobility arises when macromolecules, which are confined in narrow gallery spaces of the intercalated structure, become free to move when only confined on one side in the exfoliated structure (dynamics in half-space). For c_{CTPB} > 90 wt %, $T_{2,inter}$ increases so fast that the final value is around the $T_{2,mobile}$ value in the range of 10 ≤ c_{CTPB} ≤ 50 wt %, indicating that no CTPB molecules are constrained by clay galleries. All clay sheets are exfoliated. This agrees well with our previous rheological and SAXS studies.[65]

A turning point at c_{CTPB} = 60 wt % is also found for $T_{2,mobile}$, beyond which $T_{2,mobile}$ increases quite fast. This agrees well with the absence of a rigid component, suggests the appearance of unattached CTPB, and will be discussed with Figure 7.

Mobility Information from ^{1}H DQ Experiments. The ^{1}H DQ experiment excites double quantum coherences, which are quite sensitive to residual dipolar coupling (RDC) among protons. RDC is affected by fast local motions as well as by slow chain motions with correlation times below the time scale of the NMR experiment.[39] In this model-free approach, a homogeneous dynamic process is expected to express itself in a DQ build-up curve with a single maximum. The position of the maximum, τ_{max}, provides the characteristic time scale of the corresponding process.[47,48,50] In principle, for polymer/clay nanocomposites used in this study, a maximum at short τ_{max} suggests tightly anchored molecular segments at the clay surface. Similarly, maxima at longer τ_{max} indicate the presences of a large fraction of mobile components. DQ build-up curves with several maxima suggest heterogeneity in microstructure and the related dynamic processes.

In the following, we investigate the concentration and polymer–clay interaction dependent multimode segmental dynamics in CTPB/C_{18}–clay nanocomposites from the DQ build-up curves. Tightly anchored and intermediate components near the clay surface offered the most important message about how polymer molecules interact with clay sheets. The characteristic time τ of corresponding segmental dynamics was found to be short. In order to observe DQ signals at short τ value, a two-pulse segment (90°–τ–90°) was adopted for the excitation and reconversion of DQ signals. It was chosen for its ability to excite DQ signals among strong dipolar-coupled protons with a relatively short excitation time, τ.

Concentration Effect on CTPB/C_{18}–Clay Mobility. The ^{1}H DQ NMR spectra were measured at 30 °C for CTPB/C_{18}–clay in the entire range of polymer loadings, 0 < c_{CTPB} < 100 wt %, see Figure 4 as an example using c_{CTPB} = 60 wt %.

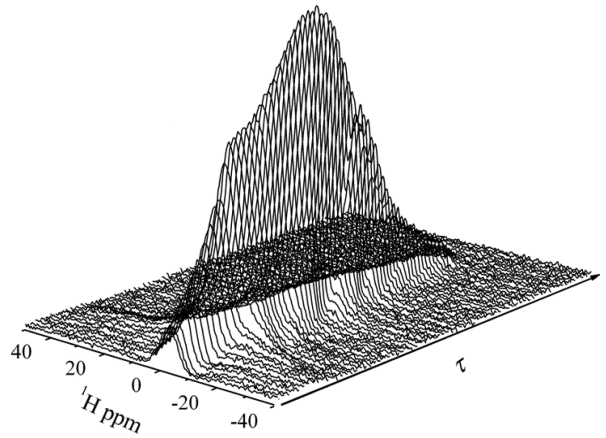

Figure 4. Typical ^{1}H DQ coherence NMR spectra of a structurally equilibrated CTPB/C_{18}–clay (c_{CTPB} = 60 wt %) nanocomposite at 30 °C.

Integration of spectra resulted in the DQ build-up curves as shown in Figure 5 for different polymer contents. The DQ build-up curves are normalized to the integral intensity of the NMR signal after a 90° pulse. The first maximum is relatively sharp, providing a well-defined value of the τ_{max}. The second and third maxima at longer τ are difficult to identify for samples with small mobile fraction because of the broadness of the signal. We prefer to plot DQ build-up curves with logarithmic abscissa, log τ, since it sharpens the peaks at long τ .

The DQ build-up curve of pure C_{18}–clay at 30 °C, Figure 5a, has a single maximum at τ_{max} =14 μs. Such single maximum is typical for component at reduced mobility such as in crystalline domains or glassy states.[48] The intensity dies off to zero at around 200 μs, suggesting that the modifier is completely immobilized by the clay surface. Below c_{CTPB} = 20 wt %, the first maximum position still remains at τ_{max} = 14 μs, indicating the same segmental immobilization near the interface for all these samples. Above c_{CTPB} = 30 wt %, the first maximum shifted to a larger τ_{max} value, indicating an increasing molecular

dx.doi.org/10.1021/jp5013472 | J. Phys. Chem. C 2014, 118, 5606–5614

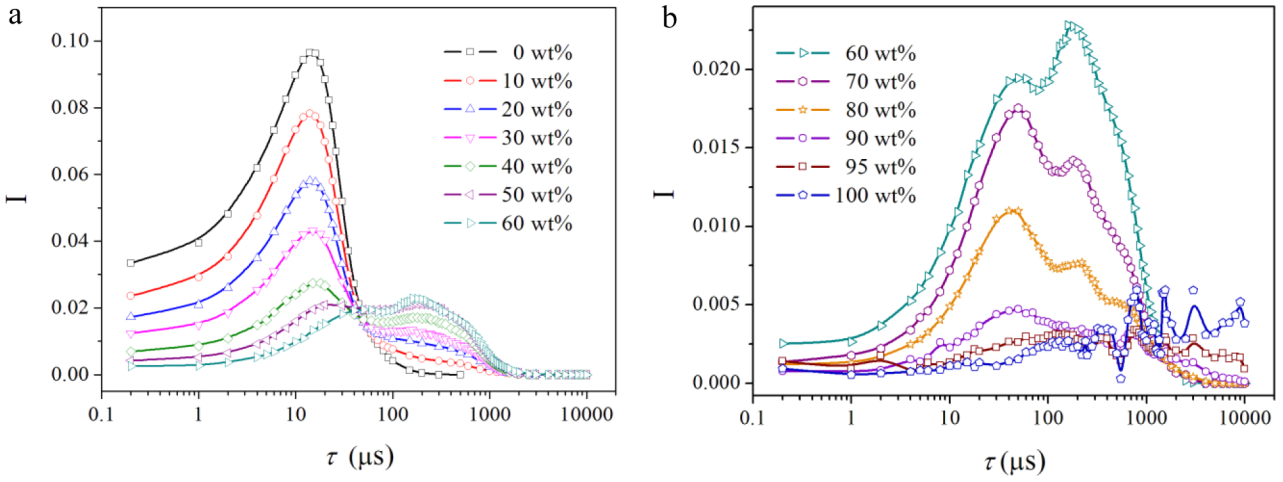

Figure 5. DQ build-up curves of CTPB/C_{18}–clay at low (a) and high (b) CTPB content. c_{CTPB} = 0 and 100 wt % referred to pure C_{18}–clay and pure CTPB, respectively. The DQ build-up curves were normalized by the integral intensity of the NMR signal after a 90° pulse.

mobility. At c_{CTPB} = 95 wt %, the first maximum is barely detectable; the fraction of modifier is too small to be detected.

With only c_{CTPB} = 10 wt %, the intensity dies off to zero after 3000 μs. We attribute the signal in the range from 200 to 3000 μs to the mobile CTPB moieties that were weakly confined on the C_{18}–clay surface. With increasing CTPB amount, the second DQ build-up maximum grew to become more obvious.

The above results indicate a concentration dependent multimode dynamics in the CTPB/C_{18}–clay nanocomposites: The first maximum at τ_{max} = 14 μs belongs to a rigid component on the clay surface, which coexisted with up to two other, progressively mobile molecular components with increasing CTPB amount.

Effect of Polymer–Clay Interaction. The polymer–clay interaction at their interface determines the exfoliation dynamics and the properties of the final nanocomposites.[2] Balazs et al. had convincingly shown that adding modifier to the clay surface or end-functionalizing the polymer will increase the interaction between polymer molecules and the clay surface, thereby lowering the systems free energy when clay sheets get separated from each other, i.e., when the clay exfoliates.[11,35] We had found a good system to adjust such interaction by adding end group on polybutadiene oligmer or modifier the MMT.[63−66,71] Previous experiments had shown that C_{18}–clay could fully exfoliate in CTPB when the c_{CTPB} exceeds 90 wt %, while at other compositions the clay only partially exfoliated or intercalated. In comparison, PB/MMT remained as a suspension of macroscopic clay particles in PB. PB/C_{18}–clay, CTPB/MMT samples reached some intermediate structure (intercalation).[63,65] The interaction strength was in the rank of CTPB/C_{18}–clay > PB/C_{18}–clay > CTPB/MMT > PB/MMT.

^{1}H DQ NMR experiments were also performed for the above-mentioned systems, including PB/C_{18}–clay, CTPB/MMT, and PB/MMT, as shown in Figure 6. Differences in polymer–clay interaction become visible when comparing DQ NMR results of Figures 5 and 6. DQ build-up curves of PB/C_{18}–clay go through a distinct maximum that was apparent at all concentrations, 10 < c_{PB} < 90 wt %, suggesting nearly homogeneous dynamics of the surface modifier of the organo–clay. For 60 < c_{PB} < 90 wt %, a soft shoulder appeared at 100 μs, which can be ascribed to weakly attached chains.

In CTPB/MMT with c_{CTPB} = 10 wt % (but not using organo–clay), the first maximum at 20 μs can be ascribed to

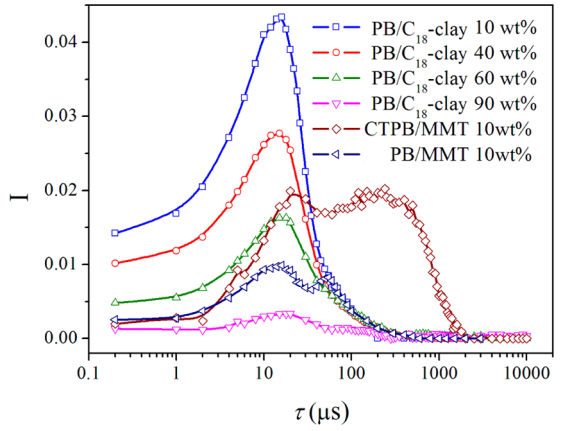

Figure 6. DQ build-up curves of PB/C_{18}–clay with c_{PB} =10, 40, 60, and 90 wt % compared to c = 10 wt % CTPB/MMT and PB/MMT.

the tightly attached CTPB on pristine clay surface, possibly comparable to the strongly immobilized EPDM chains at the surface of carbon black.[62] The tightly attached CTPB was not as solid-like as the clay surface modifier (maximum at 14 μs). A distinct second maximum appeared near τ = 800 μs, indicating the existence of loosely attached segments.

For the PB/MMT c_{PB} = 10 wt % sample, a very weak polymer–clay interaction was expected, as neither the PB has functional end groups in PB nor is there modifier on the clay surface. The first maximum occurred at the same time as for C_{18}–clay and the position of the second maximum was around 55 μs. This was ascribed to the end-functionalized effect in CTPB/MMT: the carboxyl end group in CTPB interacted more strongly with the pristine clay surface than the pure PB did. The strong interaction between the carboxyl end group and clay surface allowed more conformation freedom of the main chain and more distance between the clay surface and the main chain, while PB absorbed directly onto the clay surface in a flatter conformation as Balazs et al. had predicted earlier.[11,12,35] So the first and second τ_{max} were larger in CTPB/MMT than in PB/MMT.

Figure 7 compares the first maximum τ_{max} as function of polymer content for CTPB/C_{18}–clay and PB/C_{18}–clay. The highly mobile polymer component interacts with the clay surface and contributes to the early DQ signal. The polymer–

dx.doi.org/10.1021/jp5013472 | J. Phys. Chem. C 2014, 118, 5606−5614

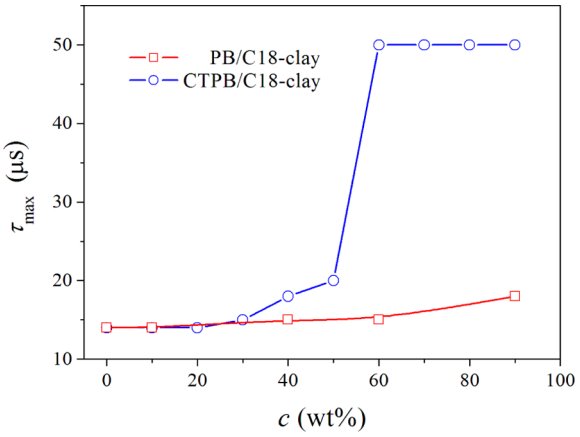

Figure 7. First τ_{max} in DQ buildup curves as a function of CTPB or PB concentrations in the CTPB/C_{18}–clay and PB/C_{18}–clay nanocomposites.

clay interaction affects the segmental dynamics and, thus, changes the τ_{max} position. In CTPB/C_{18}–clay with $0 \leq c_{CTPB} \leq 20$ wt %, τ_{max} of the rigid phase maintained its value at 14 μs. Such small τ_{max} is considered typical for highly immobilized polymer segments such as segments at the interface of semicrystalline polymers[72] and short chain fragments adjacent to the grafting sites on a silica surface.[49] Then τ_{max} begins to shift to higher values from 30 to 50 wt %. A critical value appeared at 60 wt %. Then the τ_{max} stayed constant at 50 μs up to c_{CTPB} = 90 wt %. We ascribed the critical value to the saturation of surface absorption of functionalized polymers. This critical concentration agrees well with the disappearance of the rigid fraction in Figure 3b and with our previous work,[71] in which we use a blend of end-functionalized and non end-functionalized PB to optimize the exfoliation of clay into sheets. For c_{CTPB} > 60 wt %, surface attached CTPB stayed at constant surface density. The confinement effect became nearly the same as expressed in a constant first maximum value. In comparison, for PB/C_{18}–clay, τ_{max} increased only slightly from 14 to 18 μs when increasing the PB concentration from 0 to 90 wt %, indicating there is no direct strong interaction between clay surfaces and PB chains.

The critical saturation behavior of surface adsorption plays a very important role in determining the final nanocomposite properties. Balazs et al. showed a phase transition beyond this critical value.[35,73,74] In many gel systems, the critical coverage of the clay surface is the key to better gels.[75,76] In our previous work,[71] we found a critical saturation behavior of surface adsorption of partly functionalized polymer. A molecular understanding about such critical absorption behavior could help us exfoliate clay sheets with less functionalized polymer.

Temperature Effect on C_{18}–Clay Mobility. Compatibility experiments showed that the modifier could well dissolve in the CTPB. However, at room temperature, the modifier preferred to anchor at the clay surface instead of interacting

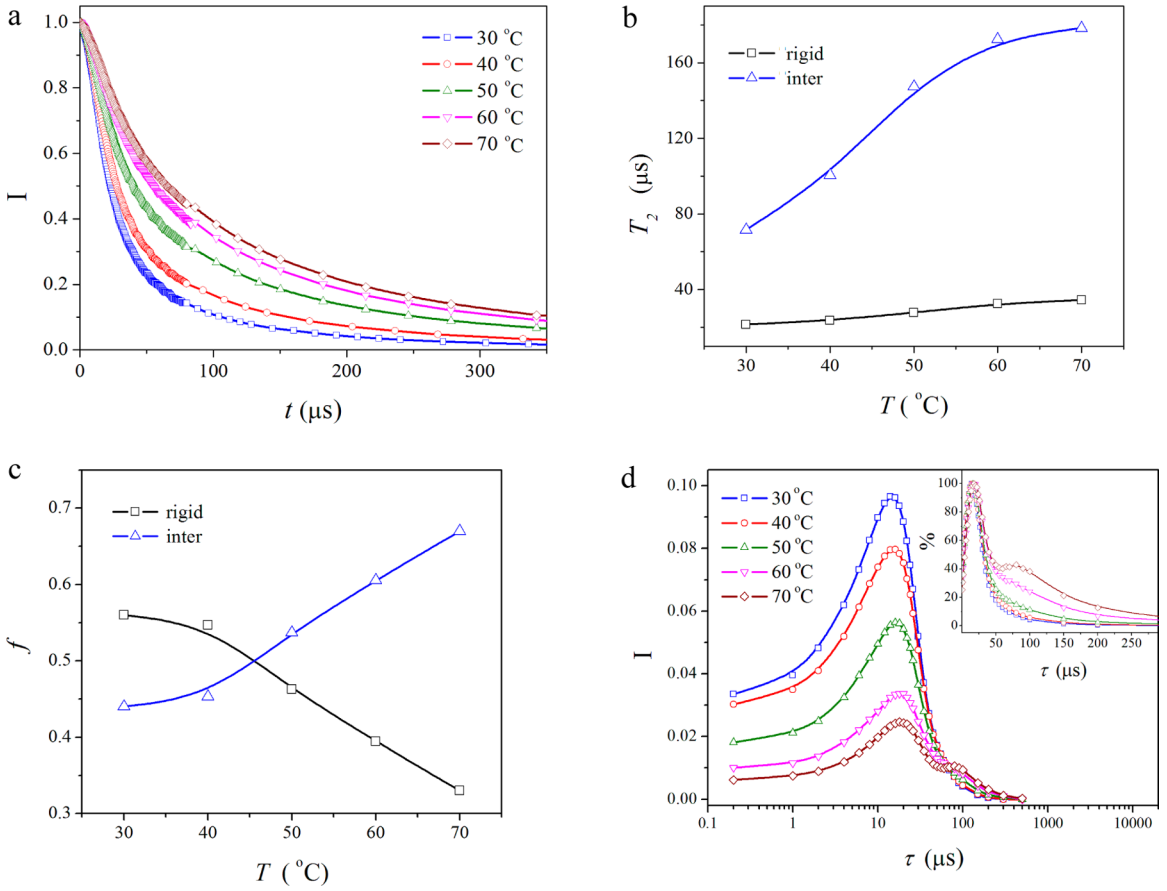

Figure 8. All data refer to pure C_{18}–clay. The temperature dependence of (a) FID, (b) T_2, (c) mobility fraction, and (d) DQ build-up curves at temperature of 30, 40, 50, 60, and 70 °C, respectively. For the sake of clarity of the relative intensity of the second maximum, an inset repeats the curves up to around 300 μs in linear scale with the intensity of the first maximum set as 100%.

dx.doi.org/10.1021/jp5013472 | J. Phys. Chem. C 2014, 118, 5606–5614

with CTPB. At temperatures above 50 °C, the modifier became more mobile and began to interact with CTPB, resulting in the exfoliated structure.[64,65] To further elucidate the temperature effect, we performed isothermal ^{1}H NMR experiments on pure C_{18}−clay at increasing temperatures, Figure 8.

The FID of pure C_{18}−clay decayed more slowly with increasing temperature, Figure 8a. With increasing temperature, $T_{2,rigid}$ increased slightly while f_{rigid} decreased slowly at first and more rapidly later. When increasing the temperature, $T_{2,inter}$ increased fast at first but then leveled off, while f_{inter} increased slowly first and fast later. The turning conditions of f_{rigid} and f_{inter} were 40 °C. The turning point of $T_{2,inter}$ was 50 °C. This means that more of the modifier becomes mobile after around 50 °C and, thus, shares surface space with CTPB so that it can anchor.

In the ^{1}H DQ NMR experiments, Figure 8d, the first maximum position only shifted slightly from 14 to 18 μs, indicating a slight increase of the mobility for the tightly anchored component. Interestingly, a shoulder appeared at 80 μs at a temperature above 50 °C. This means that the modifier on the surface of C_{18}−clay changed its mobility from homogeneous to heterogeneous because of the mobilization of the ends of the short C18 chains. This suggests that a conformation transition of the modifier happened, which potentially can strengthen the interaction of CTPB with the C_{18}−clay. This is why we found an irreversible transition at 50 °C upon heating a freshly mixed end-functionalized polybutadiene/organo−clay nanocomposites.[64,65]

DISCUSSION

A series of samples of CTPB (or PB) physically attached to the surface of C_{18}−clay were investigated by solid state ^{1}H NMR spectroscopy. By the fully refocused ^{1}H NMR FID, we quantitatively determined the fraction of the rigid, intermediate, and mobile components as well as their corresponding apparent T_2 relaxation time. By the ^{1}H DQ NMR experiments, we semiquantitatively monitor variations of the segmental dynamics at the interface for different concentrations of clay.

The structure and dynamics of organically modified clays provide useful information for the understanding the surface modifyer ("surfactant") role in the formation of nanocomposites and the effectiveness of the surface treatment.[77,78] Using FTIR, Vaia et al.[79] found the alkyl chain of the modifier behaved from solid-like to liquid-like upon heating. Panek et al.[80] found for a nanocomposite that the dynamics of the surfactant layer already changes before intercalation or exfoliation take place. Previous NMR studies have shown that the dynamics of the hydrocarbon tail in organically modified silicates was heterogeneous, both in the organically modified clay and the polymer nanocomposites with mobility enhanced with increasing distances away from the inorganic suface.[24,25] Here, our results showed that the dynamics of the modifier changed from homogeneous to heterogeneous upon heating. A partly mobile phase appeared above 50 °C which agreed with Vaia's work.[79] This mobile phase became more mobile when incorporated with CTPB. The solid-like phase at 14 μs disappeared when C_{18}−clay was saturated with CTPB.

An important feature of the dynamics of interface tethered chains is the semilocal anisotropy. Fast motions are ultimately hindered by the presence of organic−inorganic interface restrictions, and long-lived orientation correlations get induced. From the viewpoint of NMR, the CTPB/C_{18}−clay nanocomposite exhibits both liquid-like and solid-like features. Without clay, the time scales of CTPB molecular motions belong to a liquid of low elasticity. However, the presence of the interface between CTPB and C_{18}−clay prevents the chain motion from being isotropic. Thus, anisotropic spin interactions, such as the dipolar−dipolar coupling, are not completely averaged out and give rise to solid-like properties.[47] Depending on the concentration of CTPB, the strength of interfacial polymer−clay interaction, and the temperature dependence of the dynamic behaviors of modifiers, the motional restriction of the modifier and polymer could be controlled and adjusted.

The polymer content was purposely changed from low to high. The carboxyl end group anchored onto the surface first, softening the modifier. After the clay surface was saturated, CTPB partly absorbed on the surface appears, and then the free CTPB appeared. The results are in good agreement with or complementary to our previous works.[64,65]

CONCLUSIONS

A concentration and polymer−clay interaction dependent multimode segmental dynamics was found for CTPB/C_{18}−clay nanocomposites. With increasing CTPB content, discrete dynamic layers stepwise increase their segmental mobility. Three distinct types of molecular dynamics were suggested: solid like modifier and CTPB end groups anchored on the clay surface, liquid like modifier and CTPB chain next to the anchored end groups, and weakly adsorbed CTPB. The heterogeneous chain dynamics strongly depended on polymer concentration and polymer−clay interaction. The CTPB coverage of the clay surface was found to saturate at a critical value of c_{CTPB} = 60 wt %. The data also suggested c_{CTPB} = 80 wt % as the critical CTPB content at which exfoliation sets in. Above 50 °C, the modifier on the surface of C_{18}−clay was found to increase its mobility, which turned out to be a prerequisite for allowing CTPB attachment and clay exfoliation. ^{1}H DQ NMR results confirmed that the absence of the carboxyl end-group in PB or absence of the clay modifier significantly reduced the polymer−clay interaction, which was in good agreement with earlier SAXS, TEM, and rheology experiments. Based on ^{1}H DQ NMR results, a tentative model was suggested to illustrate the cooperative effect of CTPB and organo−clay in the nanocomposites.

AUTHOR INFORMATION

Corresponding Author

*Tel: 86-25-83686136. Fax: 86-25-83317761. E-mail: wangxiaoliang@nju.edu.cn.

Notes

The authors declare no competing financial interest.

ACKNOWLEDGMENTS

This work was supported by National Natural Science Foundation of China (Grant No. 21174062), the foundation research project of Jiangsu province (BK20131269), and the Program for Changjiang Scholars and Innovative Research Team in University. H.H.W. is supported by the U.S. National Science Foundation Grant No. CMMI-1334460.

REFERENCES

(1) Pinnavaia, T. J.; Beale, G. W. *Polymer-Clay Nanocomposites*; Wiley: New York, 2000.

(2) Ray, S. S.; Okamoto, M. Polymer/Layered Silicate Nanocomposites: a Review From Preparation to Processing. *Prog. Polym. Sci.* **2003**, *28*, 1539−1641.
(3) Cassagnau, P. Melt Rheology of Organoclay and Fumed Silica Nanocomposites. *Polymer* **2008**, *49*, 2183−2196.
(4) Chen, B. Q.; Evans, J. R. G. Impact Strength of Polymer-Clay Nanocomposites. *Soft Matter* **2009**, *5*, 3572−3584.
(5) Du, K.; He, A. H.; Bi, F. Y.; Han, C. C. Synthesis of Exfoliated Isotactic Polypropylene/Functional Alkyl-Triphenylphosphonium-Modified Clay Nanocomposites by in situ Polymerization. *Chin. J. Polym. Sci.* **2013**, *31*, 1501−1508.
(6) Giannelis, E. P.; Krishnamoorti, R.; Manias, E. Polymer-Silicate Nanocomposites: Model Systems for Confined Polymers and Polymer Brushes. *Adv. Polym. Sci.* **1999**, *138*, 107−147.
(7) Kuppa, V.; Foley, T. M. D.; Manias, E. Segmental Dynamics of Polymers in Nanoscopic Confinements, as Probed by Simulations of Polymer/Layered-silicate Nanocomposites. *Eur. Phys. J. E* **2003**, *12*, 159−165.
(8) Li, Y. Q.; Ishida, H. A Study of Morphology and Intercalation Kinetics of Polystyrene-Organoclay Nanocomposites. *Macromolecules* **2005**, *38*, 6513−6519.
(9) Vaia, R. A.; Giannelis, E. P. Polymer Melt Intercalation in Organically-Modified Layered Silicates: Model Predictions and Experiment. *Macromolecules* **1997**, *30*, 8000−8009.
(10) Vaia, R. A.; Giannelis, E. P. Lattice Model of Polymer Melt Intercalation in Organically-Modified Layered Silicates. *Macromolecules* **1997**, *30*, 7990−7999.
(11) Balazs, A. C.; Singh, C.; Zhulina, E. Modeling the Interactions Between Polymers and Clay Surfaces through Self-consistent Field Theory. *Macromolecules* **1998**, *31*, 8370−8381.
(12) Balazs, A. C.; Singh, C.; Zhulina, E.; Lyatskaya, Y. Modeling the Phase Behavior of Polymer/Clay Nanocomposites. *Acc. Chem. Res.* **1999**, *32*, 651−657.
(13) Krishnamoorti, R.; Vaia, R. A.; Giannelis, E. P. Structure and Dynamics of Polymer-Layered Silicate Nanocomposites. *Chem. Mater.* **1996**, *8*, 1728−1734.
(14) Manias, E.; Chen, H.; Krishnamoorti, R.; Genzer, J.; Kramer, E. J.; Giannelis, E. P. Intercalation Kinetics of Long Polymers in 2 nm Confinements. *Macromolecules* **2000**, *33*, 7955−7966.
(15) Shang, S. Y.; Fang, Z. P. Dynamics of Alpha and Alpha' Relaxation in Layered Silicate/Polystyrene Nanocomposites Studied by Anelastic Spectroscopy. *Chin. J. Polym. Sci.* **2013**, *31*, 1334−1342.
(16) Wang, K.; Liang, S.; Deng, J. N.; Yang, H.; Zhang, Q.; Fu, Q.; Dong, X.; Wang, D. J.; Han, C. C. The Role of Clay Network on Macromolecular Chain Mobility and Relaxation in Isotactic Polypropylene/organoclay Nanocomposites. *Polymer* **2006**, *47*, 7131−7144.
(17) Krishnamoorti, R.; Yurekli, K. Rheology of Polymer Layered Silicate Nanocomposites. *Curr. Opin. Colloid Interface Sci.* **2001**, *6*, 464−470.
(18) Ray, V. V.; Banthia, A. K.; Schick, C. Fast Isothermal Calorimetry of Modified Polypropylene Clay Nanocomposites. *Polymer* **2007**, *48*, 2404−2414.
(19) Vaia, R. A.; Sauer, B. B.; Tse, O. K.; Giannelis, E. P. Relaxations of Confined Chains in Polymer Nanocomposites: Glass Transition Properties of Poly(ethylene oxide) Intercalated in Montmorillonite. *J. Polym. Sci. Part B, Polym. Phys.* **1997**, *35*, 59−67.
(20) Aranda, P.; Ruizhitzky, E. Poly(ethylene oxide)-silicate Intercalation Materials. *Chem. Mater.* **1992**, *4*, 1395−1403.
(21) Wong, S.; Vaia, R. A.; Giannelis, E. P.; Zax, D. B. Dynamics in a Poly(ethylene oxide)-Based Nanocomposite Polymer Electrolyte Probed by Solid State NMR. *Solid State Ion.* **1996**, *86−8*, 547−557.
(22) Yang, D. K.; Zax, D. B. Li+ Dynamics in a Polymer Nanocomposite: An Analysis of Dynamic Line Shapes in Nuclear Magnetic Resonance. *J. Chem. Phys.* **1999**, *110*, 5325−5336.
(23) Zax, D. B.; Yang, D. K.; Santos, R. A.; Hegemann, H.; Giannelis, E. P.; Manias, E. Dynamical Heterogeneity in Nanoconfined Poly(styrene) Chains. *J. Chem. Phys.* **2000**, *112*, 2945−2951.
(24) Mao, O.; Schleidt, S.; Zimmermann, H.; Jeschke, G. Molecular Motion in Surfactant Layers inside Polymer Composites with Synthetical Magadiite. *Macromol. Chem. Phys.* **2007**, *208*, 2145−2160.
(25) Wang, L. Q.; Liu, J.; Exarhos, G. J.; Flanigan, K. Y.; Bordia, R. Conformation Heterogeneity and Mobility of Surfactant Molecules in Intercalated Clay Minerals Studied by Solid-State NMR. *J. Phys. Chem. B* **2000**, *104*, 2810−2816.
(26) Mirau, P. A.; Serres, J. L.; Jacobs, D.; Garrett, P. H.; Vaia, R. A. Structure and Dynamics of Surfactant Interfaces in Organically Modified Clays. *J. Phys. Chem. B* **2008**, *112*, 10544−10551.
(27) Borsacchi, S.; Geppi, M.; Ricci, L.; Ruggeri, G.; Veracini, C. A. Interactions at the Surface of Organophilic-Modified Laponites: A Multinuclear Solid-state NMR Study. *Langmuir* **2007**, *23*, 3953−3960.
(28) Geppi, M.; Borsacchi, S.; Mollica, G.; Veracini, C. A. Applications of Solid-State NMR to the Study of Organic/Inorganic Multicomponent Materials. *Appl. Spectrosc. Rev.* **2009**, *44*, 1−89.
(29) Anastasiadis, S. H.; Karatasos, K.; Vlachos, G.; Manias, E.; Giannelis, E. P. Nanoscopic-Confinement Effects on Local Dynamics. *Phys. Rev. Lett.* **2000**, *84*, 915−918.
(30) Schwartz, G. A.; Bergman, R.; Swenson, J. Relaxation Dynamics of a Polymer in a 2D Confinement. *J. Chem. Phys.* **2004**, *120*, 5736−5744.
(31) Hernandez, M.; Carretero-Gonzalez, J.; Verdejo, R.; Ezquerra, T. A.; Lopez-Manchado, M. A. Molecular Dynamics of Natural Rubber/Layered Silicate Nanocomposites as Studied by Dielectric Relaxation Spectroscopy. *Macromolecules* **2010**, *43*, 643−651.
(32) Malvaldi, M.; Allegra, G.; Ciardelli, F.; Raos, G. Structure of an Associating Polymer Melt in a Narrow Slit by Molecular Dynamics Simulation. *J. Phys. Chem. B* **2005**, *109*, 18117−18126.
(33) Ginzburg, V. V.; Balazs, A. C. Calculating Phase Diagrams for Nanocomposites: The Effect of Adding End-Functionalized Chains to Polymer/Clay Mixtures. *Adv. Mater.* **2000**, *12*, 1805−1809.
(34) Ginzburg, V. V.; Balazs, A. C. Calculating Phase Diagrams of Polymer-Platelet Mixtures Using Density Functional Theory: Implications for Polymer/Clay Composites. *Macromolecules* **1999**, *32*, 5681−5688.
(35) Ginzburg, V. V.; Singh, C.; Balazs, A. C. Theoretical Phase Diagrams of Polymer/Clay Composites: The Role of Grafted Organic Modifiers. *Macromolecules* **2000**, *33*, 1089−1099.
(36) Schmidt-Rohr, K.; Spiess, H. W. *Multidimensional Solid-State NMR and Polymers*; Academic Press Inc.: San Diego, CA, 1994.
(37) Baum, J.; Munowitz, M.; Garroway, A. N.; Pines, A. Multiple-Quantum Dynamics in Solid-State NMR. *J. Chem. Phys.* **1985**, *83*, 2015−2025.
(38) Munowitz, M.; Pines, A. Principles and Applications of Multiple-Quantum NMR. *Adv. Chem. Phys.* **1987**, *66*, 1−152.
(39) Saalwachter, K. Proton Multiple-Quantum NMR for the Study of Chain Dynamics and Structural Constraints in Polymeric Soft Materials. *Prog. Nucl. Magn. Reson. Spectrosc.* **2007**, *51*, 1−35.
(40) Spiess, H. W. Double-Quantum NMR Spectroscopy of Dipolar Coupled Spins under Fast Magic-Angle Spinning. In *Encyclopedia of Nuclear Magnetic Resonance*; Grant, D. M., Harris, R. K., Eds.; John Wiley & Sons, Ltd.: New York, 2002; Vol. 9, Advances in NMR, p 44.
(41) Schnell, I.; Brown, S. P.; Low, H. Y.; Ishida, H.; Spiess, H. W. An Investigation of Hydrogen Bonding in Benzoxazine Dimers by Fast Magic-Angle Spinning and Double-Quantum H-1 NMR Spectroscopy. *J. Am. Chem. Soc.* **1998**, *120*, 11784−11795.
(42) Li, B.; Xu, L.; Wu, Q.; Chen, T.; Sun, P.; Jin, Q.; Ding, D.; Wang, X.; Xue, G.; Shi, A. C. Various Types of Hydrogen Bonds, Their Temperature Dependence and Water-Polymer Interaction in Hydrated Poly(acrylic acid) as Revealed by H-1 Solid-State NMR Spectroscopy. *Macromolecules* **2007**, *40*, 5776−5786.
(43) Hou, Y. L.; Wu, Q.; Chen, T. H.; Sun, P. C. Unique Evolution of Spatial and Dynamic Heterogeneities on the Glass Transition Behavior of PVPh/PEO Blends. *Chin. J. Polym. Sci.* **2012**, *30*, 900−915.
(44) Zhu, L. L.; Gu, Q.; Sun, P. C.; Chen, W.; Wang, X. L.; Xue, G. Characterization of the Mobility and Reactivity of Water Molecules on TiO2 Nanoparticles by H-1 Solid-State Nuclear Magnetic Resonance. *ACS Appl. Mater. Interfaces* **2013**, *5*, 10352−10356.

(45) Zhang, R. C.; Yan, T. Z.; Lechner, B. D.; Schroter, K.; Liang, Y.; Li, B. H.; Furtado, F.; Sun, P. C.; Saalwachter, K. Heterogeneity, Segmental and Hydrogen Bond Dynamics, and Aging of Supramolecular Self-Healing Rubber. *Macromolecules* **2013**, *46*, 1841−1850.
(46) Graf, R.; Heuer, A.; Spiess, H. W. Chain-Order Effects in Polymer Melts Probed by H-1 Double-Quantum NMR Spectroscopy. *Phys. Rev. Lett.* **1998**, *80*, 5738−5741.
(47) Graf, R.; Demco, D. E.; Hafner, S.; Spiess, H. W. Selective Residual Dipolar Couplings in Cross-Linked Elastomers by H-1 Double-Quantum NMR Spectroscopy. *Solid State Nucl. Magn. Reson.* **1998**, *12*, 139−152.
(48) Schneider, M.; Gasper, L.; Demco, D. E.; Blumich, B. Residual Dipolar Couplings by H-1 Dipolar-Encoded Longitudinal Magnetization, Double- and Triple-Quantum Nuclear Magnetic Resonance in Cross-Linked Elastomers. *J. Chem. Phys.* **1999**, *111*, 402−415.
(49) Wang, M. F.; Bertmer, M.; Demco, D. E.; Blumich, B.; Litvinov, V. M.; Barthel, H. Indication of Heterogeneity in Chain-segment Order of a PDMS Layer Grafted onto a Silica Surface by H-1 Multiple-Quantum NMR. *Macromolecules* **2003**, *36*, 4411−4413.
(50) Jagadeesh, B.; Demco, D. E.; Blumich, B. Surface Induced Order and Dynamic Heterogeneity in Ultra Thin Polymer Films: A H-1 Multiple-Quantum NMR Study. *Chem. Phys. Lett.* **2004**, *393*, 416−420.
(51) Baum, J.; Pines, A. NMR-Studies of Clustering in Solids. *J. Am. Chem. Soc.* **1986**, *108*, 7447−7454.
(52) Saalwachter, K.; Gottlieb, M.; Liu, R. G.; Oppermann, W. Gelation as Studied by Proton Multiple-Quantum NMR. *Macromolecules* **2007**, *40*, 1555−1561.
(53) Saalwachter, K.; Herrero, B.; Lopez-Manchado, M. A. Chain Order and Cross-Link Density of Elastomers as Investigated by Proton Multiple-Quantum NMR. *Macromolecules* **2005**, *38*, 9650−9660.
(54) Saalwachter, K.; Heuer, A. Chain Dynamics in Elastomers as Investigated by Proton Multiple-Quantum NMR. *Macromolecules* **2006**, *39*, 3291−3303.
(55) Saalwachter, K.; Kleinschmidt, F.; Sommer, J. U. Swelling Heterogeneities in End-Linked Model Networks: A Combined Proton Multiple-Quantum NMR and Computer Simulation Study. *Macromolecules* **2004**, *37*, 8556−8568.
(56) Mauri, M.; Thomann, Y.; Schneider, H.; Saalwachter, K. Spin-Diffusion NMR at Low Field for the Study of Multiphase Solids. *Solid State Nucl. Magn. Reson.* **2008**, *34*, 125−141.
(57) Chambon, F.; Winter, H. H. Linear Viscoelasticity at the Gel Point of a Cross-Linking PDMS with Imbalanced Stoichiometry. *J. Rheol.* **1987**, *31*, 683−697.
(58) Winter, H. H.; Mours, M. Rheology of Polymers Near Liquid-Solid Transitions. *Adv. Polym. Sci.* **1997**, *134*, 165−234.
(59) Richter, S.; Matzker, R.; Schroter, K. Gelation studies, 4 - Why Do "Classical" Methods Like Oscillatory Shear Rheology and Dynamic Light Scattering for Characterization of the Gelation Threshold Sometimes not Provide Identical Results Especially on Thermoreversible Gels? *Macromol. Rapid Commun.* **2005**, *26*, 1626−1632.
(60) Litvinov, V. M.; Barthel, H.; Weis, J. Structure of a PDMS Layer Grafted onto a Silica Surface Studied by Means of DSC and Solid-State NMR. *Macromolecules* **2002**, *35*, 4356−4364.
(61) ten Brinke, J. W.; Litvinov, V. M.; Wijnhoven, J.; Noordermeer, J. W. M. Interactions of Stober Silica with Natural Rubber under the Influence of Coupling Agents, Studied by H-1 NMR T-2 Relaxation Analysis. *Macromolecules* **2002**, *35*, 10026−10037.
(62) Litvinov, V. M.; Orza, R. A.; Kluppel, M.; Duin, M. v.; Magusin, P. C. M. M. Rubber-Filler Interactions and Network Structure in Relation to Stress-Strain Behavior of Vulcanized, Carbon Black Filled EPDM. *Macromolecules* **2011**, *44*, 4887−4900.
(63) Chen, T. H.; Zhu, J. J.; Li, B. H.; Guo, S. Y.; Yuan, Z. Y.; Sun, P. C.; Ding, D. T.; Shi, A. C. Exfoliation of Organo−clay in Telechelic Liquid Polybutadiene Rubber. *Macromolecules* **2005**, *38*, 4030−4033.
(64) Wang, X. L.; Gao, Y.; Mao, K. M.; Xue, G.; Chen, T. H.; Zhu, J. J.; Li, B. H.; Sun, P. C.; Jin, Q. H.; Ding, D. T.; et al. Unusual Rheological Behavior of Liquid Polybutadiene Rubber/Clay Nanocomposite Gels: The Role of Polymer-Clay Interaction, Clay Exfoliation, and Clay Orientation and Disorientation. *Macromolecules* **2006**, *39*, 6653−6660.
(65) Zhu, J. J.; Wang, X. L.; Tao, F. F.; Xue, G.; Chen, T. H.; Sun, P. C.; Jin, Q. H.; Ding, D. T. Room Temperature Spontaneous Exfoliation of Organo-Clay in Liquid Polybutadiene: Effect of Polymer End-groups and the Alkyl Tail Number of Organic Modifier. *Polymer* **2007**, *48*, 7590−7597.
(66) Sun, P. C.; Zhu, J. J.; Chen, T. H.; Yuan, Z. Y.; Li, B. H.; Jin, Q. H.; Ding, D. T.; Shi, A. C. Rubber/Exfoliated-Clay Nanocomposite Gel: Direct Exfoliation of Montmorillonite by Telechelic Liquid Rubber. *Chin. Sci. Bull.* **2004**, *49*, 1664−1666.
(67) Wang, X. L.; Sun, P. C.; Xue, G.; Winter, H. H. Late-State Ripening Dynamics of a Polymer/Clay Nanocomposite. *Macromolecules* **2010**, *43*, 1901−1906.
(68) Sun, P. C.; Zhu, J. J.; Chen, T. H. 2H-NMR Characterization of Clay Dispersion and Confinement Effect on Probe Molecules in Rubber/Clay Nanocomposite-Gels. *Chin. J. Polym. Sci.* **2009**, *27*, 1−6.
(69) Li, Y. Q.; Ishida, H. Solution Intercalation of Polystyrene and the Comparison with Poly(ethyl methacrylate). *Polymer* **2003**, *44*, 6571−6577.
(70) Fechete, R.; Demco, D. E.; Blumich, B. Enhanced Sensitivity to Residual Dipolar Couplings of Elastomers by Higher-Order Multiple-Quantum NMR. *J. Magn. Reson.* **2004**, *169*, 19−26.
(71) Wang, X. L.; Tao, F. F.; Xue, G.; Zhu, J. J.; Chen, T. H.; Sun, P. C.; Winter, H. H.; Shi, A. C. Enhanced Exfoliation of Organoclay in Partially End-Functionalized Non-Polar Polymer. *Macromol. Mater. Eng.* **2009**, *294*, 190−195.
(72) Hedesiu, C.; Demco, D. E.; Kleppinger, R.; Buda, A. A.; Blumich, B.; Remerie, K.; Litvinov, V. M. The Effect of Temperature and Annealing on the Phase Composition, Molecular Mobility and the Thickness of Domains in High-Density Polyethylene. *Polymer* **2007**, *48*, 763−777.
(73) Kuznetsov, D. V.; Balazs, A. C. Phase Behavior of End-Functionalized Polymers Confined Between Two Surfaces. *J. Chem. Phys.* **2000**, *113*, 2479−2483.
(74) Kuznetsov, D. V.; Balazs, A. C. Scaling Theory for End-Functionalized Polymers Confined between Two Surfaces: Predictions for Fabricating Polymer/Clay Nanocomposites. *J. Chem. Phys.* **2000**, *112*, 4365−4375.
(75) Zebrowski, J.; Prasad, V.; Zhang, W.; Walker, L. M.; Weitz, D. A. Shake-Gels: Shear-Induced Gelation of Laponite-PEO Mixtures. *Colloid Surf. A* **2003**, *213*, 189−197.
(76) Haraguchi, K.; Farnworth, R.; Ohbayashi, A.; Takehisa, T. Compositional Effects on Mechanical Properties of Nanocomposite Hydrogels Composed of Poly(N,N-dimethylacrylamide) and Clay. *Macromolecules* **2003**, *36*, 5732−5741.
(77) Grandjean, J. Solid-State NMR Study of Modified Clays and Polymer/Clay Nanocomposites. *Clay Min.* **2006**, *41*, 567−586.
(78) Zhao, Z. F.; Tang, T.; Qin, Y. X.; Huang, B. T. Relationship Between the Continually Expanded Interlayer Distance of Layered Silicates and Excess Intercalation of Cationic Surfactants. *Langmuir* **2003**, *19*, 9260−9265.
(79) Vaia, R. A.; Teukolsky, R. K.; Giannelis, E. P. Interlayer Structure and Molecular Environment of Alkylammonium Layered Silicates. *Chem. Mater.* **1994**, *6*, 1017−1022.
(80) Panek, G.; Schleidt, S.; Mao, Q.; Wolkenhauer, M.; Spiess, H. W.; Jeschke, G. Heterogeneity of the Surfactant Layer in Organically Modified Silicates and Polymer/Layered Silicate Composites. *Macromolecules* **2006**, *39*, 2191−2200.